A Spectroscopic Study of Supported-Phosphate-Catalysts (SPCs): Evidence of Surface-mediated Hydrogen-Transfer

Daniyal Kiani[a] and Jonas Baltrusaitis*[a]

Supported-phosphate-catalysts (SPCs) are a versatile class of heterogeneous materials used in various industrially relevant processes including Fischer-Tropsch synthesis (FTS), selective catalytic reduction (SCR) of NO_x with NH_3, and Guerbet reaction of C_2H_5OH to n-C_4H_9OH. Herein, model SPCs synthesized by impregnating various supports with phosphoric acid were studied using *in-situ* chemical probe temperature-programmed-desorption infrared spectroscopy. Hydroxylation of the catalyst surface was observed during the temperature ramp on all SPCs. This behavior was not observed on the bare supports during identical experiments. The results indicate that hydroxylation of the surface occurs via sacrificial hydrogen-transfer reaction, where the chemical probe (NH_3 or C_2H_5OH) can be utilized as the hydrogen-donor. Results herein also show that the extent and the rate of hydrogen-transfer reaction depend on the identity of the support, phosphate loading, and identity of the hydrogen-donor molecule. Surface Brønsted acid sites (P–OH) do not contribute to the reaction and P=O surface sites are proposed as the active sites for the observed hydrogen-transfer. Based on the current work, it is suggested that any catalytic reaction that involves hydrogenation over phosphate-promoted or phosphate-based catalysts needs to account for the surface-mediated hydrogen-transfer capability of the phosphate sites in the overall reaction mechanism.

Introduction

Solid acid catalysts (SACs) are highly important to the chemicals industry due to their largescale use in a variety of reactions.[1] SACs have especially been heavily utilized in petroleum refining where they are employed in over 180 industrial processes.[2] Besides the petroleum refining application, SACs find use in various renewable energy and commodity chemical transformations such as the Friedel-Crafts reaction, esterification, dehydration or hydrolysis. Examples of SACs include zeolites, metal oxides, mixed metal oxides, heteropolyacids, bulk and supported phosphates and sulfates.[2] Among the reported SACs, sulfated metal oxides are the most commonly used for the reactions requiring super-acidity, but they are sensitive to moisture and unstable due to sulfur leaching.[1b] On the other hand, phosphate-based SACs are largely known to be resistant to water-poisoning and hence more desirable.[2]

Phosphate-based catalysts have also been reported to facilitate reactions where surface acidity is not necessarily critical, yet the underpinning role of the surface phosphate sites during the catalytic cycle is not fully known, as in reactions including (i) Guerbet reaction,[3] (ii) selective catalytic reduction,[4] (iii) oxidative desulfurization,[5] (iv) hydrogenation,[6] and (v) Fischer-Tropsch synthesis (FTS).[7] In this study, such catalysts are referred to as the supported phosphate catalysts (SPCs). A common trait of the catalytic reactions taking place on SPCs is the presence of hydrogenation step(s) in the overall reaction mechanism, where it can occur either via hydrogen-transfer or hydrogen-spillover depending on the hydrogen source. For example, during the Guerbet reaction of ethanol (C_2H_5OH) catalytic conversion to n-butanol (n-C_4H_9OH) over phosphate-based calcium hydroxyapatite (HAp) catalyst, a recent report showed that Meerwein–Ponndorf–Verley (MPV) type hydrogen-transfer occurred to hydrogenate butanal surface intermediate using C_2H_5OH as the sacrificial H-donor, most likely over P–OH surface sites.[3a] Likewise, during NO_x SCR with NH_3 where phosphate-promoted catalysts are also utilized,[8] it is generally accepted that hydrogen-transfer from adsorbed ammonia (NH_3*) to produce NH_2* and H* active species is one of the key steps in the overall mechanism where the transferred hydrogen reduces the active metal oxide site (M=O) to M–OH.[9] Lastly, phosphate-promoted cobalt-based catalysts are often employed for FTS using *syngas* to produce higher hydrocarbons,[7] where hydrogenation of surface adsorbed CO is a critical reaction step.[10] Little direct evidence corroborating an active role of surface phosphate sites in the hydrogen-transfer reaction can be found in the literature. In one instance, hydrogen-transfer was studied mechanistically on P=O containing moiety in a molecular complex[11] providing the first experimental evidence of reduction-coupled oxo activation (ROA) mechanism, which is similar to the proton-coupled electron transfer (PCET) mechanism.[11] Elsewhere, an IR study of SiO_2-supported phosphate catalysts reported the formation of new surface –OH sites upon NH_3 adsorption on the catalyst but did not expand upon the observed phenomenon and the underlying mechanism.[12] Therefore, it is critical to elucidate whether surface phosphate sites in SPCs can participate in hydrogenation (via hydrogen-transfer or hydrogen-spillover) since numerous reactions catalyzed by SPCs include hydrogenation step(s).[3a,7d,9,11]

[a] D. Kiani, Prof. J. Baltrusaitis
Department of Chemical & Biomolecular Engineering
Lehigh University
Bethlehem, PA-18015 (USA)
E-mail: job314@lehigh.edu

Supporting information for this article is available on the WWW under https://doi.org/10.1002/cctc.202001897

The present work generates fundamental, molecular-level insights regarding the structural dynamics and the resulting properties of SPCs via chemical probe-temperature-programmed-desorption diffuse reflectance infrared Fourier transform spectroscopy (probe-TPD-DRIFTS). Results herein provide spectroscopic evidence of surface phosphate sites participating in surface-mediated hydrogen-transfer reaction in all studied SPCs. Current results also elucidate various parameters that influence hydrogen-transfer rate over SPCs including P-loading, the identity of the support, the identity of the sacrificial H-donor molecule, and the surface acidity of the catalysts.

Experimental

Supported phosphate catalyst (SPC) synthesis

All SPCs were synthesized by impregnating ~0.5 ml aqueous H_3PO_4 solution (Sigma Aldrich, W290017-1KG-K) corresponding to 5 wt% P loading (elemental basis) onto various oxidic supports including SiO_2, Al_2O_3, TiO_2 $Zr(OH)_4$. The resulting powder was dried overnight under ambient conditions and then for 2 hr at 120 °C under air flow. Finally, the SPC was calcined at 500 °C for 5 hr before cooling to room temperature under air flow. HAp was prepared via cO–Precipitation from a solution of calcium nitrate (Sigma Aldrich, C1396-500g) and ammonium phosphate (Fisher; A684-3) where Ca/P molar ratio was ~1.67. The pH of the solution was sequentially increased to ~10 with NaOH (Merck EMSURE 1.06498.0500) so HAp precipitated out. The resulting suspension was stirred overnight before vacuum filtering. The filtered powder was dried in air at 120 °C for 2 hr and calcined in air at 500 °C for 4 hr. All supports – SiO_2: Sigma Aldrich, Davisil grade 636; 236802-100G; TiO_2: Sigma Aldrich, 232033-100G; $Zr(OH)_4$: MELcat XZO880/01, FP99999; Al_2O_3; Sasol, SBA-150 – were used as received.

In-situ DRIFTS Analysis

The *in-situ* DRIFT spectra were collected using a Thermo Nicolet iS50 FT-IR spectrometer equipped with a Harrick Praying Mantis attachment (model DRA-2) for diffuse reflectance spectroscopy. Spectra were taken using an MCT detector with a resolution of ~4 cm^{-1} and an accumulation of 96 scans. Approximately ~20 mg of each catalyst in powder form was loaded into an environmental cell (HVC-DR2, Harrick Scientific). The collection of the initial background was performed by first optimizing the beam path and IR absorption signal using the height of the full Harrick sample cup then removing the Harrick cell and placing a reflective mirror in the laser path. A spectrum was collected using the reflective mirror and was used as the background spectrum throughout the experiment. The catalysts were first cleaned of any residual hydrocarbons and dehydrated at 400 °C under 10 %O_2/N_2 gas mixture at ~30 ml/min flow rate, cooled to 120 °C under 10 % O_2/N_2 and flushed with UHP5.0 N_2 (Praxair Prospec) at 30 ml/min flow rate for ~15 minutes. Once the temperature equilibrated, the dehydrated catalyst at 120 °C was taken as then taken as the background before proceeding to adsorption. The catalysts were then subjected to adsorption at 120 °C of either 1% NH_3 in N_2 or ethanol vapor obtained using UHP5.0 N_2 at 30 ml/min flow rate bubbled through pure ethanol for ~30 minutes followed by flushing with UHP5.0 N_2 at 30 ml/min flow rate for another 30 min to remove residual physisorbed molecules. The temperature was subsequently ramped from 120 to 400 °C at 10 °C/min, while a spectrum was collected every minute.

To compare the rate of surface hydroxylation (i.e activity of various SPCs towards hydrogen-transfer), normalized absorbance for each SPC as a function of time and temperature is compared. Here, the peak intensity at t = 0 min, T = 120 °C was normalized to be 0, while the maximum peak intensity at t = 30 min, T = 400 °C for the new P–OH peak in each SPC was normalized to be 1. The normalized peak intensity is then plotted from 0 to 1 as a function of time and temperature, with the slope giving the apparent rate (min^{-1}) for P–OH evolution. By comparing the initial rate of hydroxylation (t = 0-5 mins; T = 120–170 °C), inadvertent differences and potential diffusion limitations between the various catalysts were minimized provided even at low conversion.

Results & Discussion

Nature of surface phosphate sites of SPCs via *in-situ* DRIFTS analysis

To understand how the support affects the resulting surface sites of SPCs, different support materials including SiO_2, Al_2O_3, $Zr(OH)_4$ and TiO_2 were used and contrasted with HAp-a phosphate catalyst used to catalyze Guerbet reaction, known to possess surface phosphate sites.[3a,13] Representative SPCs were prepared via incipient wetness impregnation of the pore-volume equivalent of H_3PO_4 solution onto the supports while keeping nominal P loading of 5%. *In-situ* dehydrated DRIFT spectra of bare supports and the resulting SPCs are presented in Figure 1a–e. As seen in Figure 1a, bare Al_2O_3 exhibits three major IR peaks at 3560, 3688, and 3730 cm^{-1} corresponding to hydrogen-bonded hydroxyls, HO-μ_2-Al_{VI} (type III) and HO-μ_1-Al_{VI} (type II_{66}), respectively.[14] Al_2O_3-SPC exhibits two observable peaks at 3678 and 3790 cm^{-1} due to the surface P–OH and HO-μ_1-Al_{IV} (type I_4) groups,[14a] respectively. The surface P–OH sites in HAp (Figure 1b) are evidenced by the 3674 cm^{-1} peak, while the 3568 cm^{-1} peak corresponds to both bulk and surface Ca–OH groups.[3a,15] Bare $Zr(OH)_4$ exhibits weak shoulders at 3690, 3750, and 3770 cm^{-1} corresponding to tri-bridged, bi-bridged and terminal Zr–OH groups, respectively,[16] as seen in Figure 1c. $Zr(OH)_4$-SPC exhibits two intense peaks at 3673 and 3763 cm^{-1}, tentatively assigned to surface P–OH and terminal Zr–OH groups. Bare TiO_2 (Figure 1d) exhibits one intense IR peak with two minor at 3670 cm^{-1} with shoulders at 3640 and 3695 cm^{-1}, corresponding to surface –OH from the anatase phase of TiO_2 reported in the literature.[17] TiO_2-SPC exhibits two IR peaks at 3640 and 3662 cm^{-1}, assigned to Ti–OH and P–OH groups, respectively. Lastly, as seen in Figure 1e, bare SiO_2 exhibits only one major IR peak at 3745 cm^{-1}, corresponding to terminal Si–OH groups.[18] The SiO_2-SPC contains two IR peaks at 3667 and 3745 cm^{-1}, assigned to surface P–OH and terminal Si–OH groups, respectively. Since SiO_2-SPC provides the most unequivocal band assignment of surface P–OH sites owing to the singular Si–OH IR peak at 3745 cm^{-1}, the P–OH assignment to 3667 cm^{-1} was further confirmed by varying the P-loading, where an increase in P-loading led to an increase in the 3667 cm^{-1} peak (Figure S1), corroborating the P–OH assignment. After studying the dehydrated SPC catalysts as a function of various (hydr)oxide supports, the analysis was performed to

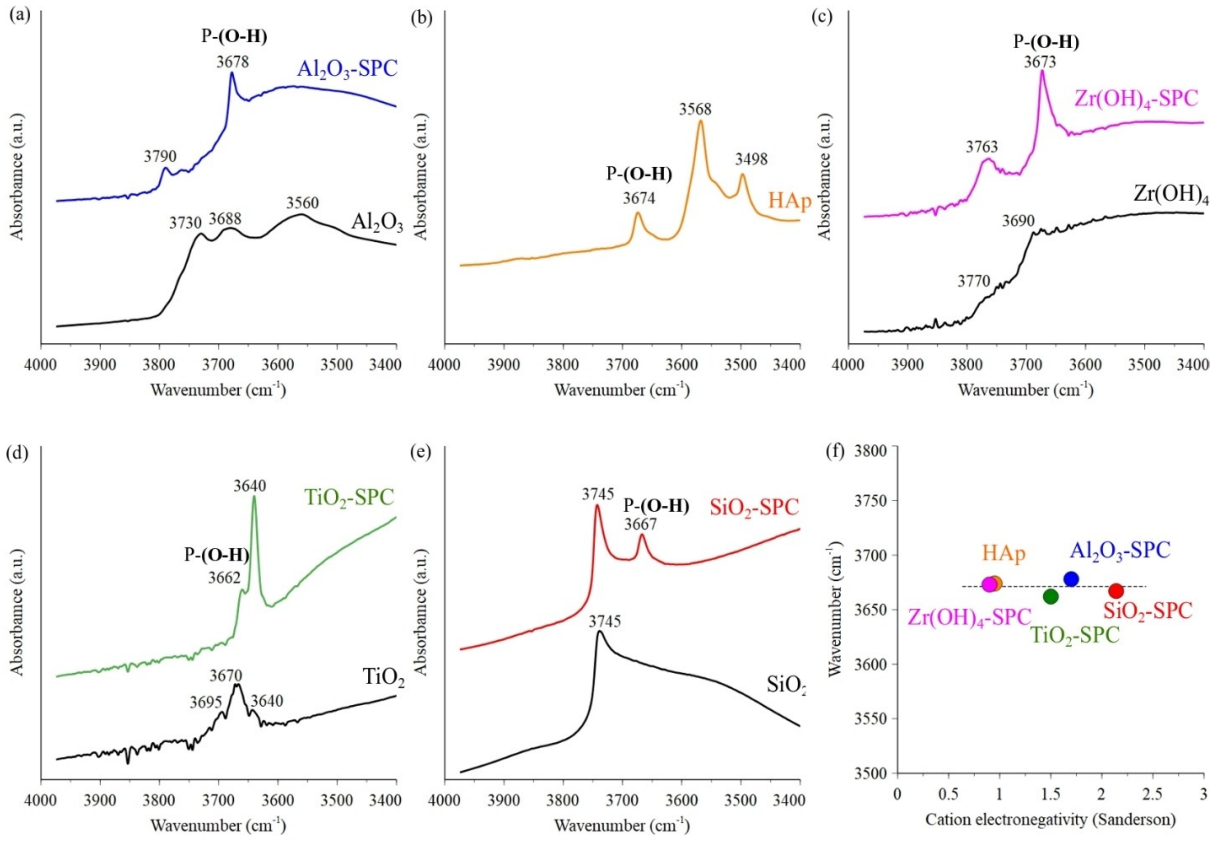

Figure 1. In-situ dehydrated DRIFT spectra taken at 120 °C after oxidative dehydration for ~1 hr at 400 °C of bare supports (black) and SPCs (colored): (a) Al_2O_3/Al_2O_3-SPC, (b) HAp, (c) $Zr(OH)_4$/$Zr(OH)_4$-SPC, (d) TiO_2/TiO_2-SPC, (e) SiO_2/SiO_2-SPC. (f) P–OH peak positions as a function of support cation electronegativity showing the absence of the correlation.

determine if electronegativity of the cation of the support an influential parameter in tuning the activity of supported heterogeneous catalysts[19] correlated with the surface P–OH IR peak position and hence the P–O–H bond length across various SPCs. As seen in Figure 1f, no correlation is observed and the P–OH IR peak position does not change systematically as the Sanderson electronegativity of the support cation increases from 0.90 (Zr^{4+}) to 2.14 (Si^{4+}). This further implies that the P–(O–H) bond lengths in each SPC do not change as a function of the support and remain relatively similar across various supports.

Next, the SPCs were probed with NH_3 to elucidate the nature of surface acid sites on these catalysts. It should be noted that the surface acid sites of the support may also contribute to the observed NH_3-DRIFTS spectra and the individual contributions from either support or the phosphate groups can not be decoupled in the IR spectra. Therefore, the general trends are discussed. As shown in Figure 2a, all SPCs exhibit Brønsted acid sites (BAS) due to P–OH and possibly X–OH where X indicates support cation, as indicated by the IR peaks due to the surface NH_4^+ at 1430–1480 cm^{-1} and 1675–1700 cm^{-1}. Moreover, besides HAp and TiO_2-SPC, other SPCs also exhibited weaker bands at ~1300–1340 and 1580–1620 cm^{-1} corresponding to surface-bound NH_3 species on Lewis acid sites (LAS). Provided that a blue-shift in the BAS and LAS peak positions is indicative of higher strength acidic sites,[20] the peak positions for LAS and BAS are plotted as a function of support cation electronegativity in Figure 2b, c, respectively. It can be seen that as the cation electronegativity increases, the LAS strength of the surface sites increases, which can either be the metal ions of the support or the unsaturated P surface sites. On the other hand, BAS strength does not exhibit a strong correlation with cation electronegativity albeit an overall increase with increasing electronegativity of the support was observed. Provided the lack of correlation between P–OH IR peak position (thus P–(O–H) bond length) and the support cation electronegativity shown in Figure 1f, the dependence of the strength of acid sites (LAS + BAS) on support cation electronegativity shown in Figure 2b--c suggests that the differences in strength are most likely due to the ligand field effects (M–O–P; M=Zr, Al, Ti, Si, Ca). A similar ligand-field effect of the support cation electronegativity on electronic structure and reactivity of surface overlayers has been reported in the literature for transition metal oxides supported on (hydr)oxide supports.[19a,d]

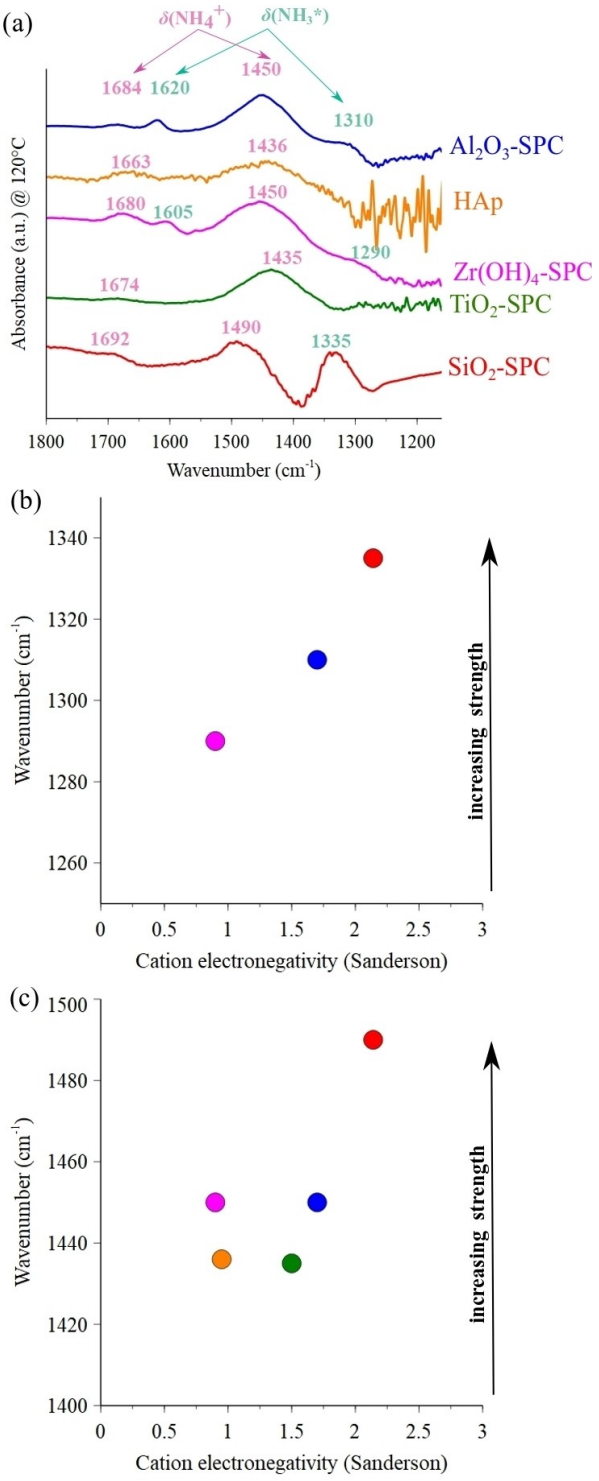

Figure 2. (a) In-situ DRIFT spectra of SPCs taken at 120 °C after NH_3 adsorption and N_2 purging. Correlation plot for (b) LAS IR peak position and (c) BAS IR peak position as a function of the support cation electronegativity. Only SiO_2, Al_2O_3 and $Zr(OH)_4$ exhibited observable IR peaks from NH_3 on LAS, other supports either had very weak LAS and/or a small population of LAS.

Spectroscopic evidence of surface hydroxylation via hydrogen-transfer during TPD DRIFTS

During NH_3-TPD-DRIFTS, the peaks arising from adsorbed NH_3 and NH_4^+ on LAS and BAS, respectively, are expected to diminish. As the temperature increases and adsorbate desorbs, the catalyst surface is also expected to lose surface –OH due to dehydration/dehydroxylation at higher temperatures. However, an interesting and unexpected phenomenon was observed upon comparing NH_3-TPD-DRIFTS for the bare supports with the corresponding SPCs, shown in Figure 3a–h. On bare supports (Figure 3. a, b, c, and d), surface dehydroxylation/dehydration occurs upon temperature ramp from 120 to 400 °C, as evident from the negative peaks marked in black. However, for all SPCs (Figure 3. e, f, g, and h), while some loss of surface –OH groups is still observed, a systematic surface hydroxylation was also observed during the temperature ramp. The IR peaks signifying this hydroxylation of the surface are marked in green and are always seen on the shoulder of the initially consumed surface –OH group (X–OH and P–OH). This behavior was also observed in the HAp catalyst, shown in Figure S2. Since the temperature ramp was conducted under the flow of inert N_2, the only source of hydrogen that could hydroxylate the surface would be the initially adsorbed NH_3/NH_4^+ species. This suggests that SPCs were able to activate the N–H bonds to transfer the hydrogen from the adsorbed species to neighboring O atoms, creating new –OH sites, which effectively serve as spectroscopic evidence of surface-mediated hydrogen-transfer reaction.

Although spectroscopic evidence is not always provided, such hydrogen-transfer phenomena were also reported recently for HAp catalyzed Guerbet reaction, where C_2H_5OH acted as the sacrificial H-donor to directly hydrogenate butanal intermediate to yield butanol product over the P–OH/OH^- surface sites.[3a,b] Likewise, K_3PO_4 solid catalysts were shown to be effective in catalyzing hydrogen-transfer from sacrificial H-donor alcohols to aldehydes and ketones via a cyclic transition state involving the surface P–OH sites.[21] Another study also provided evidence of possible involvement of surface phosphate sites in hydrogen-transfer in phosphate-promoted Pt/CeO_2 catalysts, where H_2 was used as the hydrogen source.[6a] It was shown that P-promotion led to enhanced hydrogenation at the surface sites, although the authors of that study did not expand on the mechanistic details of surface phosphate sites towards the enhancement.[6a] Based on the universally observed hydroxylation behavior upon temperature ramp, it can be argued that surface phosphate sites can transfer a hydrogen atom from adsorbed NH_3 species, which act as the sacrificial H-donor, to hydroxylate neighboring O-atoms yielding new surface –OH sites (P–OH and support–OH). This hydrogen-transfer mechanism is also corroborated by one of the most detailed reports on SiO_2-SPCs, which studied the H_3PO_4/SiO_2 system with IR spectroscopy.[12] As observed in the present study, the formation of surface –OH sites upon H_2O or NH_3 adsorption and temperature ramp was also reported, but not elaborated upon.[12]

Lastly, to understand the relative rate of surface hydroxylation via hydrogen-transfer occurring on various SPCs, the

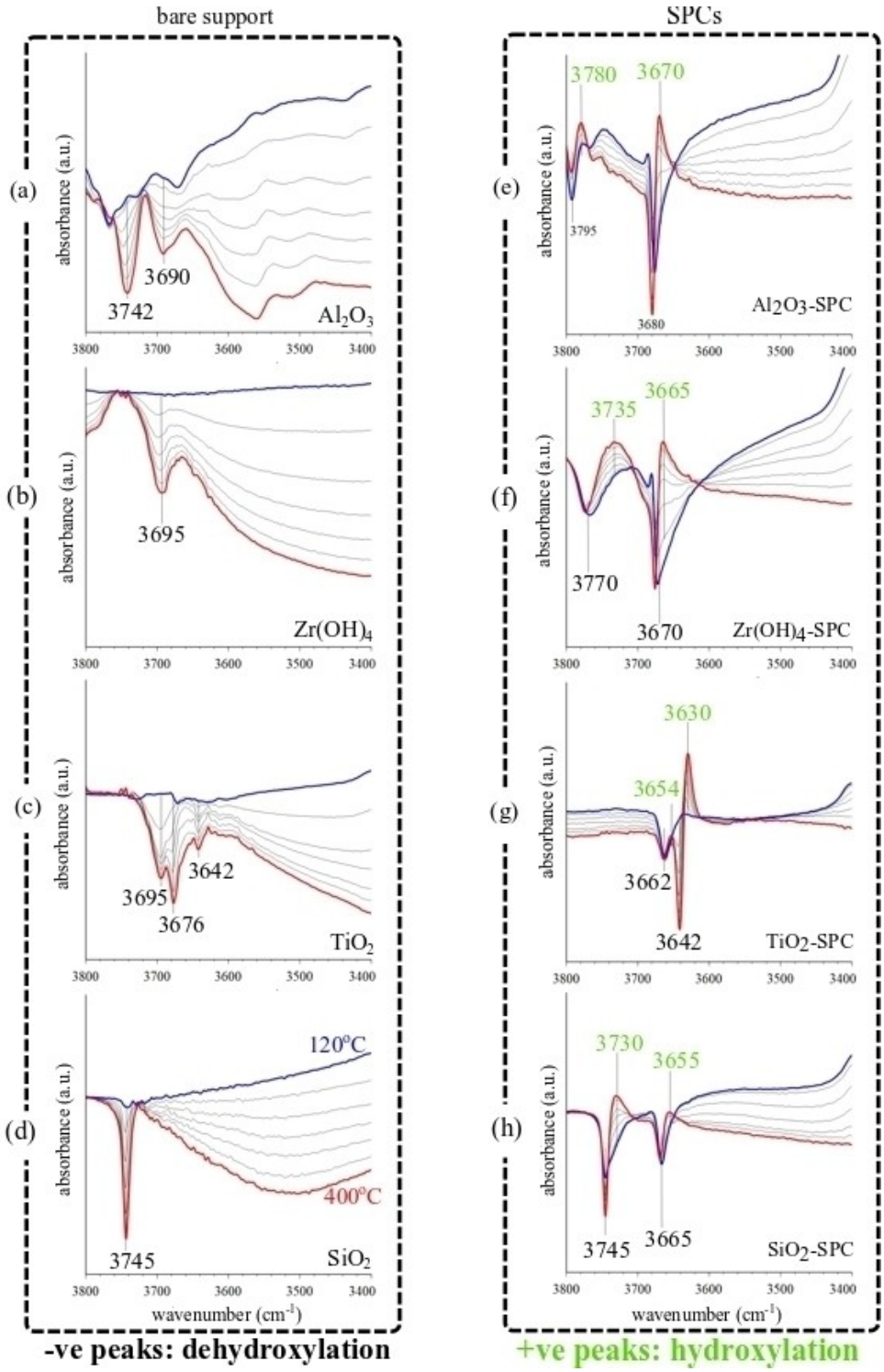

Figure 3. In-situ DRIFT spectra taken at 120 °C after NH_3 adsorption and N_2 purging during temperature ramp from 120 to 400 °C for: bare supports (a: Al_2O_3, c: $Zr(OH)_4$, e: TiO_2, g: SiO_2) and corresponding SPCs (b: Al_2O_3-SPC, d: $Zr(OH)_4$-SPC,f: TiO_2-SPC, h: SiO_2-SPC).IR peak positions marked in black signify dehydroxylation while those in green signify hydroxylation.

normalized absorbance for each SPC as a function of time and temperature was compared, shown in Figure 4a. Figure 4a suggests that the new P–OH peak growth rate (especially the initial rate of P–OH growth) proceeds fastest to slowest in the following order: $H_3PO_4/Zr(OH)_4 > HAp \sim H_3PO_4/TiO_2 > H_3PO_4/Al_2O_3 > H_3PO_4/SiO_2$. This apparent trend in the initial rate of hydroxylation going from $Zr(OH)_4$-SPC to SiO_2-SPC correlates with the Sanderson electronegativity of the support cation

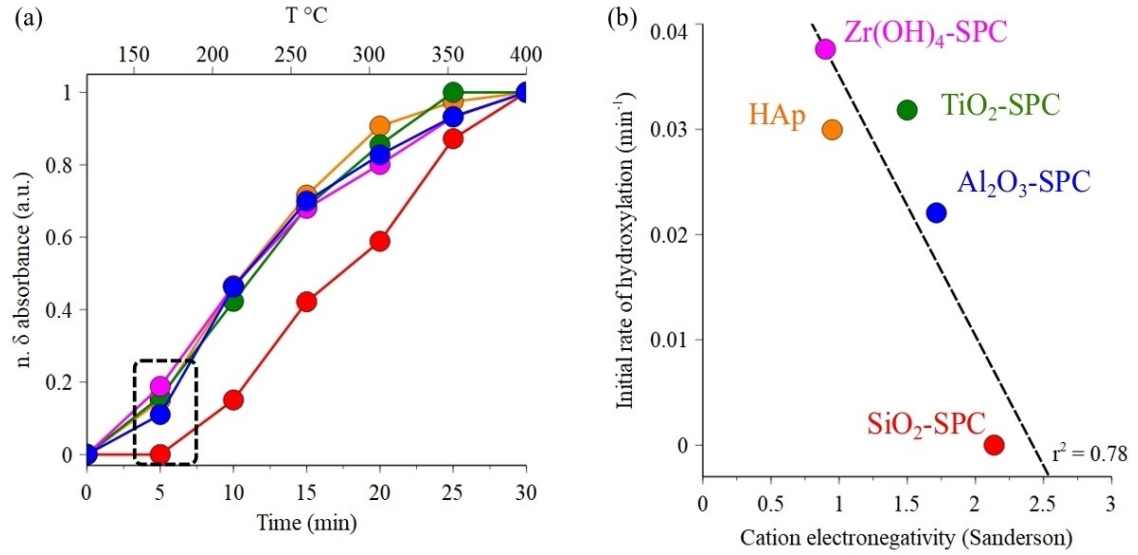

Figure 4. (a)Spectro-kinetic data for the evolution of the new P–OH peak in 3660–3690 cm^{-1} region plotted as a function of time and temperature during in-situ TPD-DRIFTS experiments. (b) Hydroxylation rate (dI/dt) is calculated by normalizing the new P–OH peak (t = 0, I = 0; t = 30 min, I = 1). The initial rate is the value of dI/dt at that time t = 5 min(170 °C).

(Figure 4b; $r^2 = 0.78$). As the electronegativity of the support cation increases, the initial rate of hydroxylation (and of hydrogen-transfer reaction) decreases linearly. The hydrogen-transfer rate trend is also opposite to the observed trend in acidic strength of surface sites; SPCs with weaker acidic sites have a faster rate of hydroxylation via hydrogen-transfer. A similar trend was reported for hydrogen-abstraction activity during methanol oxidation where supports with lower cation electronegativity yielded more active catalysts than higher electronegativity counterparts.[19a] Specifically, the more electropositive ligands (Ti–O–X and Ce–O–X where X is the identity of the active metal) exhibited higher turnover frequencies than the electronegative ligands (Al–O–X and Si–O–X).[19a] Quantum mechanical calculations in the literature further corroborated that the H-abstraction step was strongly dependent on the density of accessible electronic states in the support cation, thereby providing a possible theoretical explanation of the ligand effect.[19a] Therefore, a similar underpinning mechanism can be envisioned for SPCs where electropositive ligands (Zr–O–P, Ti–O–P, Ca–O–P) impart synergistic electronic effect in comparison to more electronegative ligands (Si–O–P) for surface phosphate sites towards hydrogen-transfer reaction.

Effect of P-loading, surface acidity and H-donor identity on hydrogen-transfer over model SiO_2-SPC

SiO_2-SPC allows unequivocal band assignment of IR peak at 3667 cm^{-1} to surface P–OH groups given that SiO_2 does not possess silanol groups that would exhibit an IR peak in that range otherwise. Therefore, various parameters that could affect the hydroxylation of the surface via the hydrogen-transfer reaction occurring during the temperature ramp were systematically studied on the model SiO_2-SPC catalysts.

Effect of P-loading

The effect of P-loading on hydroxylation behavior was studied. If hydroxylation of the surface occurs due to the surface phosphate sites, changing the P-loading would affect the degree of hydroxylation observed spectroscopically. Bare SiO_2 support, as shown in Figure 5a, does not exhibit the hydroxylation behavior observed in catalysts with the supported phosphate sites. As P-loading was increased from 0→2→5% on a P elemental basis, hydroxylation behavior increased (more intense peaks), with the new –OH groups produced as a result of the hydrogen-transfer marked in green. Moreover, a slight blue-shift was also observed in the new peaks with increasing loading, for example, the new Si–OH peak is at 3727 cm^{-1} in 2%, and 3730 cm^{-1} in 5 wt% SiO_2-SPCs. On the other hand, a slight red-shifting was observed for the new P–OH peaks with increasing wt% loading. This comparison shows that increasing P-loading in SiO_2-SPCs leads to more pronounced hydroxylation behavior during temperature ramp, further corroborating that surface phosphate sites are responsible for the hydrogen-transfer reaction leading to hydroxylation of the surface.

Effect of surface Brønsted acidity

SPCs can have various surface phosphate sites with functionalities including P–OH, P=O, P–O–P. To probe the correlation of hydroxylation via hydrogen-transfer with surface acidity (i.e. P–OH), a SiO_2-SPC was prepared where the nominal P-loading

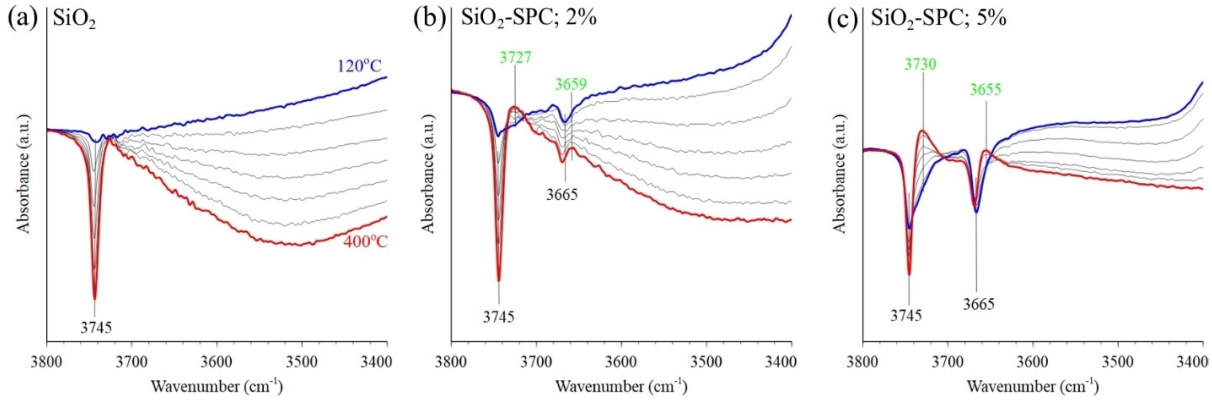

Figure 5. In-situ DRIFT spectra taken at 120 °C after NH_3 adsorption and N_2 purging during temperature ramp from 120 to 400 °C for (a) 0%, (b) 2%, (c) 5% H_3PO_4/SiO_2.

was kept constant at 5% but all acidity (Lewis + Brønsted) of the catalyst was neutralized by adding in Na^+ such that the Na/P molar ratio was 1:1. The consumption of P–OH groups upon NH_3 adsorption in SiO_2-SPC was observed in Figure 6a. However, the complete lack of Brønsted acid sites (P–OH) in the Na/P = 1 SiO_2-SPC was evident from the lack of negative peak at ~3665–3667 cm^{-1} upon NH_3 adsorption in Figure 6b. As the temperature was increased, hydroxylation was observed in both cases with the new –OH sites indicated in green. Na-poisoning of surface P–OH sites did not impact the observed surface hydroxylation via hydrogen-transfer reaction significantly, as evidenced by the new 3730 cm^{-1} IR peak in both cases. This suggests that the hydroxylation and the underlying hydrogen-transfer reaction most likely occurs over surface P=O or P–O–P sites and not on the Brønsted acidic P–OH sites. Similarly, elsewhere in the literature hydrogen-transfer was reported on a P=O moiety in a molecular complex.[11] Over the P=O containing complex, hydrogen-transfer was observed and studied mechanistically, providing first experimental evidence of reduction-coupled oxo activation (ROA) mechanism, which is similar to the proton-coupled electron transfer (PCET) mechanism.[11] Based on results in the present study and the findings from the literature, it is likely that the P=O surface sites are the active sites for the surface-mediated hydrogen-transfer reaction in SPCs.

Effect of H-donor identity (NH_3 *vs* C_2H_5OH)

The effect of utilizing a different sacrificial H-donor, C_2H_5OH, was probed next due to its relevance to SPC catalyzed Guerbet reaction. All experimental conditions and protocols were otherwise kept identical to the NH_3 case (Figure 7a). New IR peaks began to evolve adjacent to the consumed 3665 and 3745 cm^{-1} peaks from P–OH and Si–OH, respectively, during the temperature ramp, which suggests that surface hydroxyla-

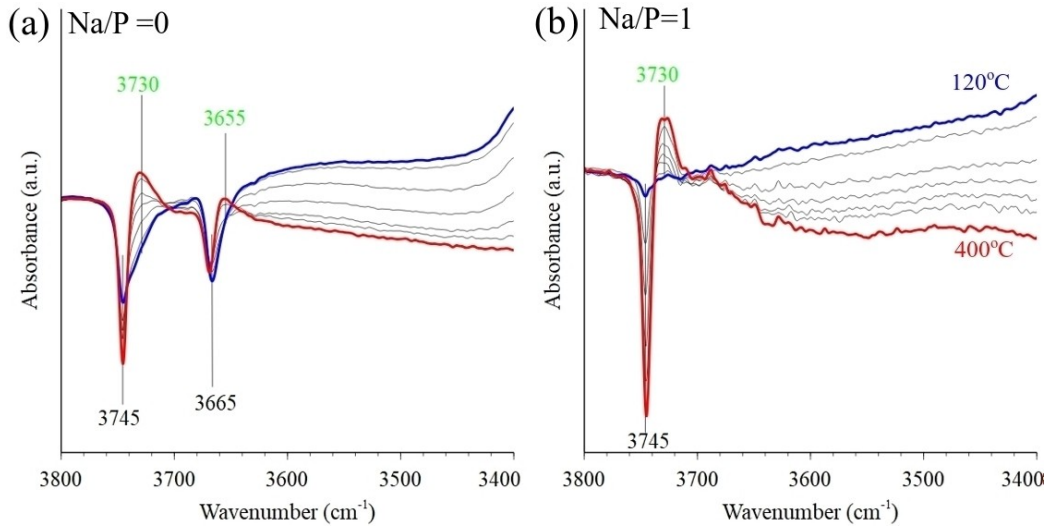

Figure 6. In-situ DRIFT spectra taken at 120 °C after NH_3 adsorption and N_2 purging during temperature ramp from 120 to 400 °C for (a) SiO_2-SPC with 5% P-loading (Na/P = 0), (b) Na-SiO_2-SPC with 5% P (Na/P = 1).

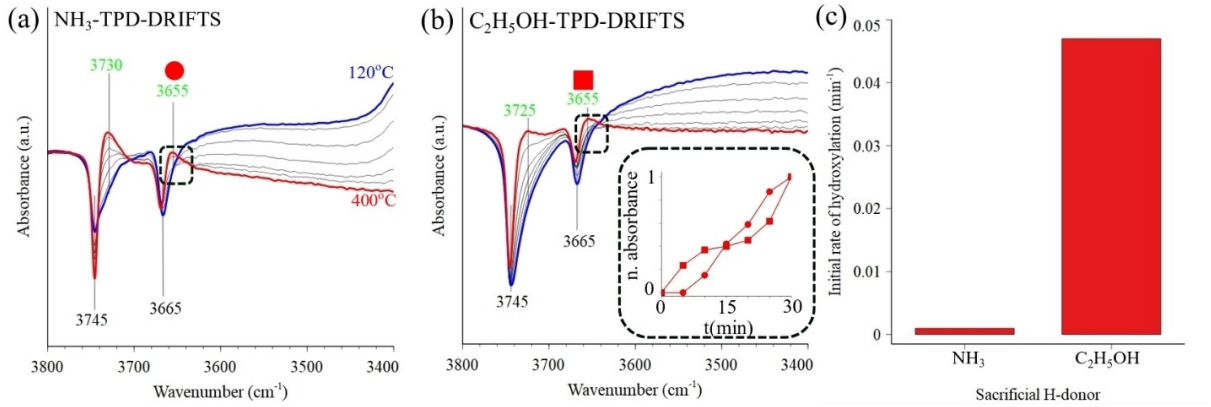

Figure 7. In-situ DRIFT spectra taken at 120 °C after (a) NH_3, (b) C_2H_5OH adsorption, followed by N_2 purging, before temperature ramped from 120 to 400 °C over SiO_2-SPC catalyst with 5 %P-loading.(c) initial rate of hydroxylation (P–OH; 3655 cm^{-1}) at t = 5 min (170 °C) as a function of different sacrificial H-donors.

tion via hydrogen-transfer was indeed occurring. To determine the difference in the initial rate of the hydrogen-transfer reaction using NH_3 and C_2H_5OH sacrificial H-donors, their initial rate of hydroxylation was extracted from normalized data for the peak growth at 3655 cm^{-1} attributed to P–OH (Figure 7c) and compared. Rate analysis indicates that the surface hydroxylation was significantly (~20 times) faster when using C_2H_5OH as the sacrificial H-donor. Since H–NH_2 dissociation energy of ~450.1 ± 0.2 $kJmol^{-1}$ and H–OCH_2CH_3 dissociation energy of ~441.0 ± 5.9 $kJmol^{-1}$ are similar, the difference in apparent initial rates is likely due to the acidity of the SPCs. The decreased rate of hydrogen-transfer is most likely due to surface poisoning from strong adsorption of basic NH_3 on surface Brønsted acid sites,[22] which does not happen during C_2H_5OH adsorption given it's less exothermic adsorption on those sites.[23] Lastly, once the sacrificial H-donor molecule has lost its H, it may desorb from the surface and/or react with the surface phosphate sites to form new functionalities. In the case of NH_3 donor, P–NH_2 may form, blocking the active sites, although exact peak deconvolution/identification remains challenging given that support–OH, support-oxide, P–O, P=O, P–OH, and NH_3 vibrations also appear in the region of interest. In the case of C_2H_5OH donor, surface ethoxy species desorb as acetaldehyde[24] or ethylene[25] and site blockage is less likely.

A perspective on the involvement of P=O surface sites in hydrogen-transfer

The hydrogen-transfer reaction dates back more than a century.[26] Hydrogen-transfer reactions are generally classified into three types: (a) hydrogen migration taking place within one molecule; (b) hydrogen disproportionation involving transfer between identical donor and acceptor units; and (c) hydrogen-transfer-dehydrogenation (HTD), occurring between a sacrificial donor and a different acceptor unit.[26] Among the three types of hydrogen-transfer reactions, HTD is by far the most important and widely used in catalysis.[26] One of the most widely known examples of an HTD reaction is the Meerwein–Ponndorf-Verley (MPV) reduction in homogeneous catalysis.[26] In the MPV reduction, aluminum alkoxide acts as a promoter for the reduction of a ketone to the corresponding alcohol in the presence of secondary alcohol as a sacrificial hydrogen donor.[26] MPV reduction of carbonyls over aluminum, zirconium, lanthanum, cerium, samarium, and ytterbium metal catalysts have been reported in the literature.[26] Unlike the homogeneous MPV reaction, MPV-type catalytic hydrogen-transfer reactions can occur over heterogeneous catalysts where a bi-functional surface is considered a requirement for the mechanism.[27] Surface acid sites are implicated in adsorbing the unsaturated molecule (usually aldehyde or ketone), while the H-donor (usually alcohol) adsorbs on the adjacent basic sites, forming a cyclic transition state containing a (P–OH) moiety during the hydrogen-transfer reaction.[27] Such MPV-type mechanisms have been hypothesized for KOH/P–OH and CaOH/P–OH pairs in phosphate-based catalysts like K_3PO_4, HAp.[3a,27]

The spectroscopic study of SPCs herein was conducted in a half-reaction mode where the SPC surface was exposed to a sacrificial H-donor like NH_3 or C_2H_5OH, but the unsaturated molecule was not introduced into the system to prolong the lifetime of surface intermediates. Moreover, no dedicated base (like K^+ or Ca^{2+}) was present in the model SPCs. Formation of new –OH surface sites (P–OH, support–OH) was observed during both NH_3-TPD-DRIFTS (Figure 1–Figure 7) and C_2H_5OH-TPD-DRIFTS (Figure 7), even when surface acid sites were poisoned with Na^+ (Figure 6). Therefore, as also shown in Figure 8, it is proposed that the active site for catalytic hydrogen-transfer is the surface P=O site, which can transfer hydrogen from an H-donor molecule,[11] yielding the new P–OH sites. The transferred H then moves onto adjacent O atoms, regenerating the P=O active site. Note that the transferred hydrogen can be quite mobile at the given temperature, as indicated by hydroxylation of the support in addition to the phosphate sites in all SPCs. Moreover, long-range hydroxylation of bare SiO_2 physically mixed with Al_2O_3-SPC during NH_3-TPD-DRIFTs (Figure S3) further corroborates that the transferred hydrogen is mobile in the 120–400 °C temperature range, in

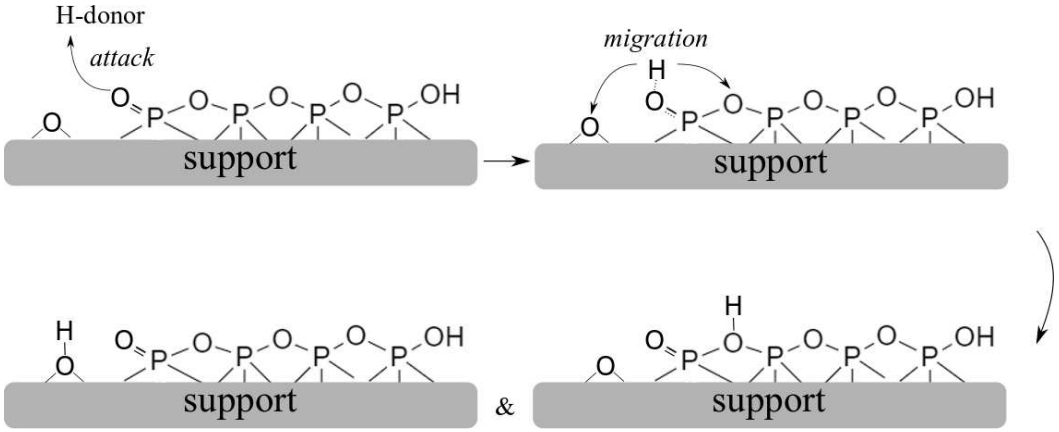

Figure 8. Schematic of simplified mechanism proposed for surface-mediated H-transfer from sacrificial H-donor over P=O sites.

agreement with conduction of H/H^+ over phosphate materials reported in the broader literature.[28] Lastly, the involvement of P=O in hydrogen-transfer is also supported by the spectro-kinetics trend; higher activity for supports with less electro-negative cations ($Zr^{4+}(OH)_4$) and low activity for supports with more electronegative cations ($Si^{4+}O_2$). P=O active sites bonded to more electronegative ligands like Si^{4+}–O–P exhibit reduced electron density in the P=O bond in comparison to Zr^{4+}–O–P, making them less basic/nucleophilic[24] and hence less active towards attacking the hydrogen of the donor molecule.[24]

Conclusion

Summarily, NH_3- and C_2H_5OH-TPD-DRIFTS results show that surface phosphate sites are involved in the surface-mediated hydrogen-transfer reaction, spectroscopically evidenced by new –OH peaks evolving in the IR spectra during temperature ramp. The hydrogen-transfer activity of various SPCs studied herein are ranked in the order of the support cation electronegativity, with higher activity for lower cation electronegativity supports ($Zr(OH)_4$) and low activity for higher cation electronegativity support (SiO_2). Other factors that influence the hydrogen-transfer activity in SPCs include P-loading and the identity of the sacrificial H-donor i.e NH_3 vs C_2H_5OH. Lastly, SPCs contain Brønsted and Lewis acid sites on the surface confirmed via NH_3-DRIFTS. However, surface acidity was shown to have little effect on the observed surface-mediated hydrogen-transfer as the Na-poisoned SiO_2-SPC was still able to exhibit comparable hydrogen-transfer despite a complete lack of surface P–OH sites. Since no other basic sites are possible, the surface P=O sites are proposed to be responsible for hydrogen-transfer from the donor molecule.

Results herein are pertinent to various industrially important catalytic chemistries including NH_3 SCR of NO_x, C_2H_5OH coupling to n-C_4H_9OH via Guerbet reaction, and FTS of higher hydrocarbons. The listed reactions not only utilize phosphate-based catalysts but also involve hydrogenation step(s) in the reaction mechanism. Current work has shown that SPCs are capable of surface-mediated hydrogen-transfer reactions in both cases, i.e with NH_3, C_2H_5OH as sacrificial hydrogen donors. Since the heterogeneous catalysis literature has largely ignored the involvement of surface P=O sites in hydrogen-transfer, the present work highlights that reaction mechanisms for catalytic reactions involving hydrogenation step(s) over phosphate-based catalysts need to be reevaluated.

Acknowledgments

This work is supported by NSF CBET 1706581. DK also gratefully acknowledges John C. Chen Endowed Fellowship for financial assistance.

Conflict of Interest

The authors declare no conflict of interest.

Keywords: DRIFTS · Hydrogen-donor · PO_x · Proton-abstraction · Transfer-hydrogenation

[1] a) W. Zhou, N. Soultanidis, H. Xu, M. S. Wong, M. Neurock, C. J. Kiely, I. E. Wachs, **2017**; b) Y. Essamlali, M. Larzek, B. Essaid, M. Zahouily, *Ind. Eng. Chem. Res.* **2017**, *56*, 5821–5832; c) J. C. Védrine, *Res. Chem. Intermed.* **2015**, *41*, 9387–9423; d) J. G. Santiesteban, J. C. Vartuli, S. Han, R. D. Bastian, C. D. Chang, *J. Catal.* **1997**, *168*, 431–441.
[2] T. Okuhara, *Chem. Rev.* **2002**, *102*, 3641–3666.
[3] a) S.-C. Wang, M. C. Cendejas, I. Hermans, *ChemCatChem* **2020**, *12*, 4167–4175; b) Z. D. Young, R. J. Davis, *Catal. Sci. Technol.* **2018**, *8*, 1722–1729; c) L. Silvester, J.-F. Lamonier, J. Faye, M. Capron, R.-N. Vannier, C. Lamonier, J.-L. Dubois, J.-L. Couturier, C. Calais, F. Dumeignil, *Catal. Sci. Technol.* **2015**, *5*, 2994–3006; d) D. Gabriëls, W. Y. Hernández, B. Sels, P. Van Der Voort, A. Verberckmoes, *Catal. Sci. Technol.* **2015**, *5*, 3876–3902; e) J. T. Kozlowski, R. J. Davis, *ACS Catal.* **2013**, *3*, 1588–1600; f) T. Tsuchida, J. Kubo, T. Yoshioka, S. Sakuma, T. Takeguchi, W. Ueda, *J. Catal.* **2008**, *259*, 183–189.
[4] a) W. Li, S. Jin, R. Zhang, Y. Wei, J. Wang, S. Yang, H. Wang, M. Yang, Y. Liu, W. Qiao, L. Ling, M. Jin, *RSC Adv.* **2020**, *10*, 12908–12919; b) G. Zhang, X. Huang, Z. Tang, *Molecular Catalysis* **2019**, *478*, 110562; c) K. Xie, K. Leistner, K. Wijayanti, A. Kumar, K. Kamasamudram, L. Olsson,

Catal. Today **2017**, *297*, 46–52; d) F. Li, Y. Zhang, D. Xiao, D. Wang, X. Pan, X. Yang, *ChemCatChem* **2010**, *2*, 1416–1419.
[5] P. Zhang, L. Kang, M. Zhu, B. Dai, *Sustain. Energy Fuels* **2020**, *4*, 4293–4300.
[6] a) Y. Ma, B. Chi, W. Liu, L. Cao, Y. Lin, X. Zhang, X. Ye, S. Wei, J. Lu, *ACS Catal.* **2019**, *9*, 8404–8412; b) Y. M. Park, D. H. Lee, Y. J. Lee, H.-S. Roh, C.-H. Chung, J. Wook Bae, *ChemCatChem* **2019**, *11*, 1707–1721.
[7] a) M. Martinelli, M. Kumaran Gnanamani, S. D. Hopps, D. E. Sparks, A. MacLennan, Y. Hu, B. H. Davis, G. Jacobs, *ChemCatChem* **2018**, *10*, 3709–3716; b) S.-J. Park, J. M. Cho, C.-I. Ahn, Y.-J. Lee, K.-W. Jun, B. G. Cho, J. W. Bae, *J. Mol. Catal. A* **2017**, *426*, 177–189; c) M. K. Gnanamani, G. Jacobs, U. M. Graham, V. R. R. Pendyala, M. Martinelli, A. MacLennan, Y. Hu, B. H. Davis, *Appl. Catal. A* **2017**, *538*, 190–198; d) M. H. Woo, J. M. Cho, K.-W. Jun, Y. J. Lee, J. W. Bae, *ChemCatChem* **2015**, *7*, 1460–1469.
[8] a) Y. You, C. Shi, H. Chang, L. Guo, L. Xu, J. Li, *Molecular Catalysis* **2018**, *453*, 47–54; b) T. Yan, Q. Liu, S. Wang, G. Xu, M. Wu, J. Chen, J. Li, *ACS Catal.* **2020**, *10*, 2747–2753.
[9] a) Y. Yang, J. Liu, F. Liu, Z. Wang, J. Ding, H. Huang, *Chem. Eng. J.* **2019**, *361*, 578–587; b) N. R. Jaegers, J.-K. Lai, Y. He, E. Walter, D. A. Dixon, M. Vasiliu, Y. Chen, C. Wang, M. Y. Hu, K. T. Mueller, I. E. Wachs, Y. Wang, J. Z. Hu, *Angew. Chem. Int. Ed.* **2019**, *58*, 12609–12616; c) J.-K. Lai, I. E. Wachs, *ACS Catal.* **2018**, *8*, 6537–6551.
[10] W. Chen, I. A. W. Filot, R. Pestman, E. J. M. Hensen, *ACS Catal.* **2017**, *7*, 8061–8071.
[11] J. Chu, T. G. Carroll, G. Wu, J. Telser, R. Dobrovetsky, G. Ménard, *J. Am. Chem. Soc.* **2018**, *140*, 15375–15383.
[12] M. J. D. Low, P. Ramamurthy, *J. Phys. Chem.* **1968**, *72*, 3161–3167.
[13] M. Ben Osman, S. Diallo-Garcia, V. Herledan, D. Brouri, T. Yoshioka, J. Kubo, Y. Millot, G. Costentin, *J. Phys. Chem. C* **2015**, *119*, 23008–23020.
[14] a) X. Liu, *J. Phys. Chem. C* **2008**, *112*, 5066–5073; b) X. Liu, R. E. Truitt, *J. Am. Chem. Soc.* **1997**, *119*, 9856–9860.
[15] I. M. Hill, S. Hanspal, Z. D. Young, R. J. Davis, *J. Phys. Chem. C* **2015**, *119*, 9186–9197.
[16] M. McEntee, G. W. Peterson, A. Balboa, I. Iordanov, R. B. Balow, P. E. Pehrsson, *J. Phys. Chem. C* **2019**, *123*, 17205–17213.
[17] H. Lin, J. Long, Q. Gu, W. Zhang, R. Ruan, Z. Li, X. Wang, *Phys. Chem. Chem. Phys.* **2012**, *14*, 9468–9474.
[18] a) A. Comas-Vives, *Phys. Chem. Chem. Phys.* **2016**, *18*, 7475–7482; b) E. L. Lee, I. E. Wachs, in *The Journal of Physical Chemistry C, Vol. 111*, American Chemical Society, **2007**, pp. 14410–14425.
[19] a) L. J. Burcham, M. Badlani, I. E. Wachs, *J. Catal.* **2001**, *203*, 104–121; b) M. Zacharska, A. L. Chuvilin, V. V. Kriventsov, S. Beloshapkin, M. Estrada, A. Simakov, D. A. Bulushev, *Catal. Sci. Technol.* **2016**, *6*, 6853–6860; c) K.-i. Shimizu, A. Satsuma, *Energy Environ. Sci.* **2011**, *4*, 3140–3153; d) K.-I. Tanaka, A. Ozaki, *J. Catal.* **1967**, *8*, 1–7.
[20] a) C. D. Baertsch, S. L. Soled, E. Iglesia, *J. Phys. Chem. B* **2001**, *105*, 1320–1330; b) G. Busca, *Phys. Chem. Chem. Phys.* **1999**, *1*, 723–736.
[21] R. Radhakrishan, D. M. Do, S. Jaenicke, Y. Sasson, G.-K. Chuah, *ACS Catal.* **2011**, *1*, 1631–1636.
[22] V. Agarwal, H. Metiu, *J. Phys. Chem. C* **2015**, *119*, 16106–16114.
[23] K. Alexopoulos, M.-S. Lee, Y. Liu, Y. Zhi, Y. Liu, M.-F. Reyniers, G. B. Marin, V.-A. Glezakou, R. Rousseau, J. A. Lercher, *J. Phys. Chem. C* **2016**, *120*, 7172–7182.
[24] E. Baráth, *Catalysts* **2018**, *8*.
[25] L. K. Freydlin, A. M. Levit, *Bulletin of the Academy of Sciences of the USSR, Division of chemical science* **1952**, *1*, 177–184.
[26] D. Wang, D. Astruc, *Chem. Rev.* **2015**, *115*, 6621–6686.
[27] M. J. Gilkey, B. Xu, *ACS Catal.* **2016**, *6*, 1420–1436.
[28] a) P. G. M. Mileo, T. Kundu, R. Semino, V. Benoit, N. Steunou, P. L. Llewellyn, C. Serre, G. Maurin, S. Devautour-Vinot, *Chem. Mater.* **2017**, *29*, 7263–7271; b) T. Omata, T. Yamaguchi, S. Tsukuda, T. Ishiyama, J. Nishii, T. Yamashita, H. Kawazoe, *Phys. Chem. Chem. Phys.* **2019**, *21*, 10744–10749; c) Y. Jin, Y. Shen, T. Hibino, *J. Mater. Chem.* **2010**, *20*, 6214–6217; d) T. Yamaguchi, Y. Saito, Y. Kuwahara, H. Yamashita, T. Ishiyama, J. Nishii, T. Yamashita, H. Kawazoe, T. Omata, *J. Mater. Chem. A* **2017**, *5*, 12385–12392.

Manuscript received: November 25, 2020
Revised manuscript received: January 11, 2021
Accepted manuscript online: January 19, 2021
Version of record online: February 17, 2021